

RSC Advances



This is an *Accepted Manuscript*, which has been through the Royal Society of Chemistry peer review process and has been accepted for publication.

Accepted Manuscripts are published online shortly after acceptance, before technical editing, formatting and proof reading. Using this free service, authors can make their results available to the community, in citable form, before we publish the edited article. This *Accepted Manuscript* will be replaced by the edited, formatted and paginated article as soon as this is available.

You can find more information about *Accepted Manuscripts* in the [Information for Authors](#).

Please note that technical editing may introduce minor changes to the text and/or graphics, which may alter content. The journal's standard [Terms & Conditions](#) and the [Ethical guidelines](#) still apply. In no event shall the Royal Society of Chemistry be held responsible for any errors or omissions in this *Accepted Manuscript* or any consequences arising from the use of any information it contains.

Visual detection of *Maize chlorotic mottle virus* using unmodified gold nanoparticles

Zhanmin Liu^{a1}, Xueying Xia^a, Cuiyun Yang^b, Lin Wang^a

^a School of Life Sciences, Shanghai University, Shanghai, P.R.C, 200444, China;

^b Shanghai Entry-Exit Inspection and Quarantine Bureau, Shanghai 200135, China

Abstract:

Maize chlorotic mottle virus causes corn lethal necrosis disease, and can transmit via infected maize seeds. It remains a challenge to detect this virus to prevent its introduction and infection and spread transmission fields. For this purpose, visual detection of *Maize chlorotic mottle virus* was investigated in cooperation with unmodified gold nanoparticles (AuNPs). Detection relies on the fact that the dispersed AuNPs solution is red due to the intense surface plasmon absorption band at 520 nm, whereas the AuNPs solution in the presence of the species-specific probes and RT-PCR target products of *Maize chlorotic mottle virus* is grey blue after saline induction. After optimization of the size of AuNPs, concentration of NaCl, probes in reaction system and evaluation of specificity and sensitivity of a novel assay, visual detection of *Maize chlorotic mottle virus* using unmodified AuNPs has been developed with simple preparation of samples in our study. Through this assay, as low as 30 pg/ μ L of RNA of *Maize chlorotic mottle virus* were thus detected visually, by the naked eye, without the need for any sophisticated, expensive instrumentation and biochemical reagents. The specificity was 100% and exhibited good reproducibility in 15 sample viruses. The results indicate that this assay is highly species-specific, simple, low-cost, and visual for easy detection of *Maize chlorotic mottle virus* in plant tissues. Therefore, visual detection of *Maize chlorotic mottle virus* is a potentially useful tool for middle or small-scales corporations and entry-exit inspection and quarantine bureau to detect *Maize chlorotic mottle virus* in maize seeds or plant tissues.

Keywords: Visual detection; *Maize chlorotic mottle virus*; Gold nanoparticles

Introduction

Maize chlorotic mottle virus (MCMV) is the sole species in the genus *Machlomo virus* (family Tombusviridae), and it is the single strand RNA virus. As an important plant pathogenic virus, MCMV was first reported infecting *Zea mays* in Peru¹ where it caused losses of 10-15% in floury and sweet corn cultivars. The combination of MCMV with the *Maize dwarf mosaic virus*, *Sugarcane mosaic virus*, or *Wheat streak mosaic virus* may also give rise to severe reaction known as maize lethal necrosis². In addition, this virus can be introduced readily into other countries by seeds or vectors^{3,4}. Because of the potential threat to the production of maize crops, it was listed as a quarantine pest by the Chinese government in 2007, and was identified in maize seeds imported from the United States, Germany, and Mexico, indicating a high risk of MCMV introduction with the increasing international exchange of maize seeds. In order to prevent introduction of MCMV through international exchange of maize seeds, there is imperative to develop a reliable and sensitive assay for detection of MCMV. At present, many kinds of assays have been employed for detection of MCMV, including biological indexing⁵, ELISA², electron

¹Corresponding author. Zhanmin Liu, School of Life sciences, Shanghai University, 333 Nanchen Road, Shanghai, 200444, China. Tel.: +86-21-66135166; Fax: +86-21-66135166.
E-mail: zhmliu@shu.edu.cn

microscopy⁶, a real-time RT-PCR⁷ and surface plasmon resonance⁸. However, biological indexing is time-consuming, labor-intensive and requires greenhouse space; the results of ELISA are dependent on the quality and availability of expensive antibodies; electron microscopy, real-time RT-PCR and surface plasmon resonance require very expensive equipment; RT-PCR is the requirement of running gels increases the risk of contamination during post-PCR manipulations.

Colorimetric assay is a simple, and a direct visual detection without the need for any complicated equipment^{9,10}. Gold nanoparticles (AuNPs) have been used as sensing material for colorimetric detection of some chemical and biomolecules (such as glucose¹¹, protein¹², Dopamine¹³, Interleukin-6¹⁴, and cholesterol¹⁵) due to their unique optical properties^{16, 17}. It presents a color change of AuNPs colloids based on electrostatic interaction between AuNPs with nucleotide sequences. Therefore, AuNPs can be selectively aggregate owed to the different characteristics of the single and double strand DNA, and provide a simple, inexpensive and colorimetric detection of various DNA sequences^{18,19} and RNA sequence²⁰, and have been used to detection of *Acinetobacter baumannii* and *Mycobacterium tuberculosis*^{21,22}. However, many color assays are time-consuming due to about a two-day's preparation for modified AuNPs. In order to overcome the limitation, a reliable, simple, cost-effective, and visual detection of MCMV using unmodified gold nanoparticles has been developed in the study.

Experimental

Reagents and materials

Carnation ringspot virus (CRSV), *Odontoglossum ringspot virus* (ORSV), *Cucumber green mottle mosaic virus* (CGMMV), *Lily symptomless virus* (LSV), *Cymbidium mosaic virus* (CymMV), *Southern bean mosaic virus* (SBMV), *Bean pod mottle virus* (BPMV), *Maize chlorotic mottle virus* (MCMV) were supplied by Shanghai Entry-Exit Inspection and Quarantine Bureau, Shanghai, China. *Staphylococcus aureus* and *Listeria monocytogenes* were maintained in our laboratory. H₂AuCl₄ (99.999%) and sodium citrate dehydrate were purchased from Sinopharm Group Chemical Regent Co., Ltd., Shanghai, China. All glasses were cleaned in aqua regia (3 parts HCl, 1 part HNO₃) rinsed with pure H₂O. The species-specific fragment from *Staphylococcus aureus* (289 bp) and the species-specific fragment from *Listeria monocytogenes* (226 bp) were supplied by our laboratory and used as controls. All oligonucleotides used for the study were synthesized and purified by Sangon Biotech.

Methods

Extraction of Genomic DNA and RNA

For DNA isolation, 1 ml of overnight pure culture LB broth was centrifuged and washed once with physiologic saline. Genomic DNA was isolated from the pellet using the TIANamp Bacteria DNA Kit (TianGenBiotech, Beijing, China) according to the manufacturer's instructions and dissolved in ddH₂O.

Viral genomic RNA was extracted from 100 mg of leaves infected with the virus, respectively using TIANamp Virus RNA Kit (Beijing, China) according to the manufacturer's instructions. The

RNA was eluted with 60 μ L of elution buffer and stored at -80°C pending analysis.

PCR for Control DNA

The 289 bp fragment from *Staphylococcus aureus* and 226 pb fragment from *Listeria monocytogenes* were used to be controls and prepared according to our previous research^{23, 24}.

RT-PCR

In order to amplify the species-specific fragment for MCMV, the primers and probe designed according to Genbank X14736 were synthesized as follows: F: 5'-TCAGGTTTCATGCCCTCT-3', R: 5'-ATGCTTGCTCCATCCACT-3'. RT-PCRs were conducted in the two-step reactions by using a Mastercycler gradient thermal cycler (Eppendorf, Foster City, Calif.). For cDNA synthesis, reaction mixture (10 μ L) was prepared with 1.0 μ L of RNA template, 7.0 μ L of RNase-Free H₂O and 2.0 μ L of 5 \times g DNA Buffer, and then the mixture was kept 42 $^{\circ}\text{C}$ for 3 min. Subsequently, 2.0 μ L of 10 \times Fast RT Buffer, 1.0 μ L of Enzyme Mix, 0.5 μ L of reverse primer, and 6.5 μ L of RNase-Free H₂O were added into the above mixture (10 μ L), mixed completely, and incubated 42 $^{\circ}\text{C}$ for 22 min, and 95 $^{\circ}\text{C}$ for 3 min to synthesize cDNA. For target sequences amplification, PCR was carried out in a 50 μ L reaction mixture composed of 5.0 μ L of 10 \times Taq DNA polymerase buffer, 6.0 μ L of 2.5 mmol/L dNTPs, 1.0 μ L of Taq DNA polymerase, 1.0 μ L of primer and reverse primer, 35 μ L of ddH₂O and 1.0 μ L of cDNA. PCR reaction was performed in an Eppendorf gradient thermocycler. The cycling procedures for amplifying target sequence were set as follows: an initial step of denaturation at 94 $^{\circ}\text{C}$ for 2 min; 30 cycles of denaturation at 94 $^{\circ}\text{C}$ for 30 s, anneal at 55 $^{\circ}\text{C}$ for 30 s and elongation at 72 $^{\circ}\text{C}$ for 1 min; final extension at 72 $^{\circ}\text{C}$ for 10 min. 5.0 μ L of RT-PCR product was analyzed by gel electrophoresis using a 1.5% agarose gel containing 0.5 μ g of EB dye. The running conditions were constant voltage at 120 V for 30 min. After electrophoresis, the relative amount of PCR products were analyzed by image analysis software (Quantity OneTM, Bio-Rad, CA, USA). The 600 bp DNA markers, which contain 600, 500, 400, 300, 200, and 100 bp DNA fragments, served as standards for the evaluation of the gel electrophoresis results. The expected PCR product is the length of 475 bp.

Preparation of AuNPs

AuNPs with the average diameter of 13 nm were synthesized by a citrate reduction method²⁵. Briefly, AuNPs were prepared by boiling an aqueous solution of 0.01% HAuCl₄ (100 ml) under rapid stirring and adding 3.5 ml of 1% sodium citrate. After 15 min of boiling and further 30 min of rapid stirring, the solution was allowed to be cooled to room temperature and filtered through a 0.8 μ m membrane. Concentration of the as-prepared AuNPs was estimated to be 3.5 nM, which was calculated from the quantity of starting material (HAuCl₄) and the size of the nanoparticles. The synthesized colloidal AuNPs used had an average diameter of about 13 \pm 2 nm as determined by transmission electron microscopy (TEM) (Fig.1C).

Verification experiments for the visual detection strategy

After 2 μ L of 10 mM probe (5'-CCACATTCATGTTCCGTGT-3') and 2 μ L of target sequences (RT-PCR products) were mixed completely in the sterile microtube, the mixture was kept 94 $^{\circ}\text{C}$ for 2 min, 55 $^{\circ}\text{C}$ for 6 min and then cooled to room temperature for 15 min. With addition of 60 μ L of AuNPs into the mixture, the solution maintained for 90 min. afterwards, 6 μ L of PBS was

added into the mixture and the total volume of mixture reached 70 μL before the mixture was determined by transmission electron microscopy and UV-vis absorption spectrum over the wavelength ranging from 400 nm to 800 nm. The control experiment was the same as previous protocol except that a target sequence was replaced with 289-bp fragments from *Staphylococcus aureus*.

Critical concentration of NaCl on the color change of the complex of AuNPs with DNA

In order to achieve the Critical NaCl concentration to the complex of AuNPs with DNA, Four different concentration of NaCl were induced in to the complex of AuNPs with double strand DNA, single strand DNA (probe) respectively.

Specificity of visual detection of MCMV

1 μL of 10-fold diluted RT-PCR product and 1 μL of 10 mM probe were mixed completely in a sterile PCR tube. The mixture was denatured at 95 $^{\circ}\text{C}$ for 2 min, annealed at 55 $^{\circ}\text{C}$ for 6 min, and then cooled to room temperature for 10 min. After addition of 30 μL of colloidal AuNPs to the reaction mixture, and 0.34 μL of ddH₂O, the total volume reached 32.34 μL and kept for 90 min at room temperature, finally, 2.66 μL of 0.5 M PBS buffer was added into the mixture. The color changes in the solutions were observed visually and recorded by cameras. There existed 60 mM Na⁺ in the final mixture. To validate the specificity of this method, 15 sample viruses were tested using the above procedure.

Sensitivity of visual detection of MCMV

The sensitivity of the assay was evaluated by performing the above procedure in a series of diluted RNA of MCMV.

Results

The design of visual detection of MCMV based on AuNPs colorimetric assay

The detection strategy is shown in Scheme 1. Single strand DNA (ssDNA) adsorbs on citrate-coated AuNPs, and this adsorption increases the negative charge on the AuNPs, which leads to increasing repulsion between the particles^{26,27}. The adsorption of ssDNA on AuNPs occurs due to the fact that ssDNA can uncoil and expose its nitrogenous bases, and the attractive electrostatic forces between the bases and the AuNPs allow adsorption of the ssDNA. On the other hand, double strand DNA (dsDNA) does not adsorb on AuNPs owed to the repulsion between its negatively charged phosphate backbone and the negatively charged coating of citrate ions on the surfaces of the AuNPs²⁶. Therefore, when AuNPs are added to a saline solution containing the target DNA and its complementary, specific probes, AuNPs aggregate (since the probes are not free to stabilize the AuNPs) and the solution color changes to grey blue. However, in the absence of the target or the presence of a noncomplementary target, the probes remain free to stabilize the AuNPs thus preventing their aggregation, and the solution color remains red (Scheme.1). The denaturation and annealing help species-specific probes sufficiently absorb the targets. In appearance, the color difference of AuNPs can indicate whether the RT-PCR product can combine complementally with species-specific probe or not, and identified the samples.

Verification experiments for the visual detection strategy

Various states of AuNPs with different DNA under the saline induction were recorded respectively and shown (Fig.1). When AuNPs with probes (ssDNA) and nontarget DNA were induced under the saline solution, they were disperse, stable and red [Fig.1A(c), and Fig.1C(c)], and the absorption peak of them was still 520 nm [Fig.1B(c)], which was the same as the only AuNPs. Otherwise, after the saline induction, AuNPs with probes and target DNA were aggregation and grey blue [Fig.1A(b), and Fig.1C(b)], and the absorption peak at 520 nm decreased and a new peak at about 650 nm appeared [Fig.1B(b)], implying that the AuNPs were aggregated. The results are exactly consistent with the visual detection strategy and showed the strategy is valid.

Critical NaCl concentration on color change of the complex of AuNPs colloid

Single strand DNA probes can absorb into the surface of AuNPs through electric interaction to increase the stability of colloidal of AuNPs, and the electric double layers of colloidal of AuNPs can also retain good stability^{26,27}. However, there exist a critical salt concentration, which can induce the complex of AuNPs with double strand DNA to deposit, but the complex of AuNPs with probes is still steadily stable. As shown in Fig.2, the color of four samples was clearly red at the concentration of NaCl below 60 mM (Fig.2A, B), however, the color of three samples turned to grey blue at the concentration of NaCl over 60 mM (Fig.2 D), only one sample was grey blue and others appeared red color (Fig.2C), this results demonstrated that the critical concentration of NaCl was 60 mM, which was sufficient for aggregation of AuNPs and guaranteed the color change of visual detection.

Specificity of visual detection of MCMV

Based on our previous similar strategy and results^{19,28}, a species-specific sequence was used to be a novel molecular marker for detection of MCMV (supplement data), and RT-PCR product was expected as the 476-bp fragments. As we supposed that all of MCMV (8 viruses) could be carried out reverse transcript PCR and gain about 476-bp fragments in lane 1-8 in Fig.3A according to our designing specific primers and simultaneously, other nonMCMV (7 viruses) cannot be successfully amplified in lane 9-17 in Fig. 3A with the same primers, the results showed that the novel molecular marker and the RT-PCR assay are high species-specific to MCMV.

The color change is the prominent indicator which determines the accuracy of the visual detection of MCMV assay. In the experiment, there were numerous nonspecific amplifications based on negative controls. Simultaneously there existed some specific amplification because of MCMV. The RT-PCR of negative controls could not combine with the specific probe because that there was lack of target templates in lane 9-16 in Fig. 3B, which lead to free probes to absorb on the surface of AuNPs, increased NaCl resistance, and prevented the aggregation of AuNPs induced by NaCl, and the color in mixtures is always red in lane 0, and 9-16 in Fig. 3B. On the other hand, specific probes and the specific amplifications hybridized polymeric substance in lane 1-8 in Fig. 3B, which lead to absence of probes, thus AuNPs could not be protected from salt induction to cause aggregation, and the color changed grey blue in lane 1-8 in Fig. 3B. Compared with RT-PCR assay, visual detection assay was high species-specific to MCMV; In addition, only 0.1 μ L of RT-PCR product in visual detection assay could make the same detection conclusion as the 5 μ L of RT-PCR assay, which indicated that visual detection assay was more high sensitive.

High sensitivity of the visual detection assay

In order to know the sensitivity of this new colorimetric assay system, RT-PCR was performed on decreasing amounts of RNA. As shown in Fig. 4B, mixtures of extensively amplified target, probes and AuNPs (lanes 1-5), changed gray blue after salt addition. Simultaneously, in cases where minimal RNA amplification yields could not appear in electrophoresis (lanes 6-9) in Fig. 4A, the solutions retained the red color after salt addition. The color differences among the various concentrations of RNA were clearly distinguishable owing to the strong aggregation of AuNPs occurring in the solution not containing enough templates. The observations described that as few as 30 pg/ μ L of the RNA of MCMV could be detected by observing the color change arising during the extended incubation time of 90 min following salt addition, it suggested that over the 30 pg/ μ L RNA temple could amplify enough specific RT-PCR product to combine with the specific probes, so that there were not adequate free probes to prevent from strong aggregation of AuNPs after salt induction. The result implied the extent of amplification dominated the sensitivity of this colorimetric RNA detection methodology. Thus, an increase in RT-PCR efficiency through optimization of experimental conditions might bring about a more obvious and drastic color change even when less RNA is used. In addition, 0.1 μ L of RNA used in visual detection method had the consistent results with 5 μ L of RNA used in RT-PCR, which indicated the visual detection of MCMV was more sensitive than RT-PCR.

Discussion

In general most researchers have used the coat protein genes as molecular markers for various viruses²⁹⁻³¹; however, moving protein gene has been used as markers for *Cucumber green mottle mosaic virus*^{32, 33}, which implies that some sequences in genome are possible to be molecular markers for virus and bacterium. In fact, the signal transduction gene, *vicK* has been identified as a molecular marker for detection of *Staphylococcus aureus*²³ and Lmo0460 sequence has been identified as a molecular marker for detection of *Listeria monocytogenes* in our previous research based on comparative genome and sequences alignment analysis¹⁹. With the similar strategy, 600 bp of sequence (X14736) has been identified as a novel molecular marker for detection of MCMV by means of bioinformatics. Simultaneously, RT-PCR also confirmed the result in our study.

The nano-gold assay is extremely affected by main factors including ssDNA concentration and length, salt concentration, AuNP concentration, shape and size, denaturation/annealing temperature, the hybridization buffer³⁴. Of these, the constant parameters in this study were the ssDNA (probes) length, AuNP concentration, denaturation/annealing temperature, the hybridization buffer, which helps the visual detection assay for practice application.

Particle size of AuNPs affects the visual detection³⁴. Control of the particles size, shape and charge was achieved by using the appropriate concentration of the sodium citrate, which acts as reducing and capping agent²¹. The experimental results showed that 13 nm AuNPs provide more consistent detection result compared with larger AuNPs (23 nm) because the stability of AuNPs decreases with the increase of particle's size resulting in easy aggregation. Thus, 13 nm AuNPs was selected for all experiments.

High temperature can result in AuNPs aggregation. However, in this assay, AuNPs is added after the annealing step, which enabled the use of optimal temperature for annealing without interference with AuNPs solution stability.

Although the pH of the reaction affects the aggregation of AuNPs³⁵, the reaction solution is the special buffer and provides a stable pH without interference with the aggregation of AuNPs in this

assay.

NaCl concentration is an important contributor to affect the color of AuNPs colloidal solution. Although single strand DNA probes adsorb on AuNPs to help them more stable and prevent their aggregation, the increase in NaCl concentration will destroy gradually the double electrostatic layer of AuNPs, and once NaCl concentration reaches its critical value, AuNPs will aggregate unavoidably, and the solution turns blue. Certainly, the critical concentration of NaCl can vary according to various target, probes and AuNPs.

Except for NaCl concentration, the concentrations of the probes also affect the AuNPs state. In the presence of target, a very high probe concentration will not be only hybrid with the target, and the rest of probes can adsorb the surface of AuNPs to prevent aggregation leading to a false negative result. On the other hand, in the absence of target low concentration probes adsorb AuNPs, and excess AuNPs will be aggregate after salt induction leading to a false positive result. Consequently, the optimal probe concentration was found to be 10 μM in the total assay volume.

The denaturation and annealing steps are deemed necessary before the addition of the AuNPs to increase the specificity of the assay, this because that the extent of RT-PCR targets combination with the species-specific probe is the key of the successful assay, and increasing the time of the denaturation and annealing steps also increases the percentage of positive results. In our opinion, increasing the time of denaturation and annealing might increase the probability of the probes annealing specifically to species-specific RT-PCR products in MCMV, hence, after adding the species-specific probes to RT-PCR products, the mixture was subjected to denaturation at 95 $^{\circ}\text{C}$ for 2 min, annealing at 55 $^{\circ}\text{C}$ for 6min, and then cooling to room temperature for 10 min in our experiment.

Modified AuNPs with the thiol-functionalized oligonucleotide probes for colorimetric detection of single base mismatch in DNA sequence have been reported according to the color change of solution due to the cross-linking reaction between nanoparticles³⁶, however, differently modified AuNPs for different targets are required, separation of ligands for modified AuNPs (such as DNA) can be costly; covalent conjugation of ligands onto the surface of AuNPs is a tedious and time-consuming process (1–2 days). Unmodified AuNPs can solve these problems. Unmodified AuNPs are prepared through the classical citrate reduction process and are loosely capped by negatively charged citrates. As a result, they show high affinity to flexible, positively charged molecules but much less affinity to rigid, negatively charged ones³⁷.

The method for RNA extracting from plant tissues is a conventional protocol, many kits for isolation of RNA from plant tissues are used in commercial activities. Any kits can be available in our assay once they can extract genomic RNA from plant tissues.

RT-PCR is the requirement of running gel, which increases the risk of contamination during post-PCR manipulations, this is because that ethidium bromide (EB) is to act as a mutagen, and harmful operators. Before running gel is performed, EB must be added into gel so that it combines the DNA to light under a UV lamp. Therefore, EB contaminates the environment. However, our methodology does not require EB to cause light, and the color change depends on the states of AuNPs. So, our assay is safer comparing with RT-PCR.

China has strengthened the prevention and control of introduction of maize seed through

international exchange of maize seeds, there is seldom report MCMV transition, therefore, it is very difficult to gain field isolates, and this is why only one field isolate was used in the study. This assay only required simple sample preparation and the results were obtained in a few hours, which make it a promising assay. Since we did not have access to field isolates, the current method has only been tested on the limited number of known MCMV isolate. Therefore, attempts have been made to obtain more trials with field isolated viruses to tump fundamentals for assay applications.

In recent year, severe chlorotic mottle symptoms found in sweat corns or sugarcans were observed at the base of infected leaves with MCMV in many countries and regions³⁸⁻⁴⁰. Sugarcane and corn in field were also found to be infected with MCMV in Yunnan province, China in 2013. The novel assay for detection MCMV is very suitable for the detection field leaves samples according to only our sample preparation and RT-PCR protocol.

To our knowledge, this is the first approach employing the probe for visual detection of MCMV using unmodified AuNPs. The new method requires only addition of AuNPs with the solution after RT-PCR. All of plant tissues including maize seeds or leaves need completely crushed and total genome is extracted, and these protocols are very common and conventional. Surface modification of AuNPs is not required. Although it still requires a RT-PCR step, post-PCR analysis such as gel electrophoresis is eliminated in this method. As a consequence of its simplicity, the methodology should find wide application in assays performed in small-scale corporations or in developing countries, where only a thermal cycler and nonhighly trained personnel need to be available. In addition, this method has the potential of being incorporated into a portable sensor system, such as a micro-fluidic device or a diagnostic kit.

Conclusion

In this work, we took full advantage of interaction AuNPs with nucleic acids and developed a low-cost, facile, sensitive method for visual detection of MCMV with the unmodified AuNPs. The assay described is easily readout with the naked eye. In comparison with other methods for detection of MCMV, the method is more attractive because of its high sensitivity, low-cost, ready availability and simple manipulation. This is the first application of the unmodified AuNPs-based biosensing platform for detection of MCMV.

Acknowledgements

This research was financed by the grants from Science Project of General Administration of Quality Supervision, Inspection and Quarantine of the People's Republic of China (2014IK014), and Natural Science Foundation of Shanghai (15ZR1415600)

References

1. J. Castillo and T. T. Hebert, *Fitopatologia*, 1974, **9**, 79-84.
2. J. X. Wu, Q. Wang, H. Liu, Y. J. Qian, Y. Xie and X. P. Zhou, *J. Zhejiang Univ. Sci. B*, 2013, **14**, 555-562.
3. D. Cabanas and A. Bressan, *Phytopathology*, 2011, **101**, S24-S24.
4. D. Cabanas, S. Watanabe, C. H. V. Higashi and A. Bressan, *J. Econ. Entomol.*, 2013, **106**, 16-24.

5. J. K. Uyemoto, *Plant Dis.*, 1983, **67**, 7-10.
6. F. J. Morales, J. A. Arroyave, J. Castillo and C. De Leon, *Maydica*, 1999, **44**, 231-235.
7. Y. J. Zhang, W. J. Zhao, M. F. Li, H. J. Chen, S. F. Zhu and Z. F. Fan, *J. Virol. Methods*, 2011, **171**, 292-294.
8. C. Zeng, X. Huang, J. M. Xu, G. F. Li, J. Ma, H. F. Ji, S. F. Zhu and H. J. Chen, *Anal. Bioche.*, 2013, **440**, 18-22.
9. D. Y. Zhang, W. D. Zhang, X. P. Li and Y. Konomi, *Gene*, 2001, **274**, 209-216.
10. D. Y. Zhang and B. Liu, *Expert Rev. Mol. Diagn.*, 2003, **3**, 237-248.
11. Q. Q. Sun, Y. N. Yu, J. J. Li and S. J. Bao, *Rsc. Adv.*, 2015, **5**, 34486-34490.
12. L. Shastri, H. N. Abdelhamid, M. Nawaz and H. F. Wu, *Rsc. Adv.*, 2015, **5**, 41595-41603.
13. Q. T. Huang, X. F. Lin, C. Q. Lin, Y. Zhang, S. R. Hu and C. Wei, *Rsc. Adv.*, 2015, **5**, 54102-54108.
14. J. F. Huang, H. Chen, W. B. Niu, D. W. H. Fam, A. Palaniappan, M. Larisika, S. H. Faulkner, C. Nowak, M. A. Nimmo, B. Liedberg and A. I. Y. Tok, *Rsc. Adv.*, 2015, **5**, 39245-39251.
15. X. Ou, X. R. Tan, X. F. Liu, H. M. Chen, Y. Fan, S. H. Chen and S. P. Wei, *Rsc. Adv.*, 2015, **5**, 66409-66415.
16. W. Zhao, M. A. Brook and Y. F. Li, *Chembiochem*, 2008, **9**, 2363-2371.
17. M. Szemes, P. Bonants, M. de Weerd, J. Baner, U. Landegren and C. D. Schoen, *Nucleic Acids Res.*, 2005, **33**, e70.
18. J. L. Ma, B. C. Yin and B. C. Ye, *Rsc. Adv.*, 2015, **5**, 65437-65443.
19. Z. M. Liu, J. C. Zhu, C. Y. Yang and X. H. LI, *Anal. Methods*, 2015, 8159-8164.
20. F. Liu, G. M. Xiang, L. Q. Zhang, D. N. Jiang, L. L. Liu, Y. Li, C. Liu and X. Y. Pu, *Rsc. Adv.*, 2015, **5**, 51990-51999.
21. M. A. F. Khalil, H. M. E. Azzazy, A. S. Attia and A. G. M. Hashem, *J. Appl. Microbiol.*, 2014, **117**, 465-471.
22. M. M. Hussain, T. M. Samir and H. M. E. Azzazy, *Clin. Biochem.*, 2013, **46**, 633-637.
23. Z. M. Liu, X. M. Shi and F. Pan, *Diagn. Micr. Infect. Dis.*, 2007, **59**, 379-382.
24. B. Hang and Z. M. Liu, *Food Science (in chinese)* 2009, 197-200.
25. K. C. Grabar, R. G. Freeman, M. B. Hommer and M. J. Natan, *Anal. Chem.*, 1995, **67**, 734-743.
26. H. X. Li and L. Rothberg, *P.N.A.S.*, 2004, **101**, 14036-14039.
27. H. X. Li and L. J. Rothberg, *J. Am. Chem. Soc.*, 2004, **126**, 10958-10961.
28. Z. M. Liu, X. M. Shi and F. Pan, *Diagn Microbiol Infect Dis*, 2007, **59**, 379-382.
29. G. A. Barthe, T. L. Ceccardi, K. L. Manjunath and K. S. Derrick, *J. Gen. Virol.*, 1998, **79**, 1531-1537.
30. T. Moravec, N. Cerovska and N. Boonham, *J. Virol. Methods*, 2003, **109**, 63-68.
31. A. I. Bhat, V. Bhadramurthy, S. Siju and P. S. Hareesh, *J. Plant Biochem. Biotechn.*, 2006, **15**, 33-37.
32. X. N. Li and X. P. Ren, *Acta. Phytopylacica Sinica*, 2009, 283-284.
33. X. Wu and Y. M. Deng, *J. Yangzhou Univ. (Agri. & Life Sci. Ed.) (in chinese)*, 2010, 75-80.
34. S. Teepoo, P. Chumsaeng, K. Palasak, N. Bousod, N. Mhadbamrung and P. Sae-Lim, *Talanta*, 2013, **117**, 518-522.
35. L. Li and B. X. Li, *Analyst*, 2009, **134**, 1361-1365.
36. C. A. Mirkin, R. L. Letsinger, R. C. Mucic and J. J. Storhoff, *Nature*, 1996, **382**, 607-609.

37. S. He, D. B. Liu, Z. Wang, K. Y. Cai and X. Y. Jiang, *Sci. China Phys. Mech.*, 2011, **54**, 1757-1765.
38. Q. Wang, X. P. Zhou and J. X. Wu, *Plant Dis.*, 2014, **98**, 572-573.
39. M. Lukanda and A. Owati, *Plant Dis.*, 2014, **98**, 1448-1449.
40. T. C. Deng, C. M. Chou, C. T. Chen, C. H. Tsai and F. C. Lin, *Plant Dis.*, 2014, **98**, 1748-+.

Figure Captions:

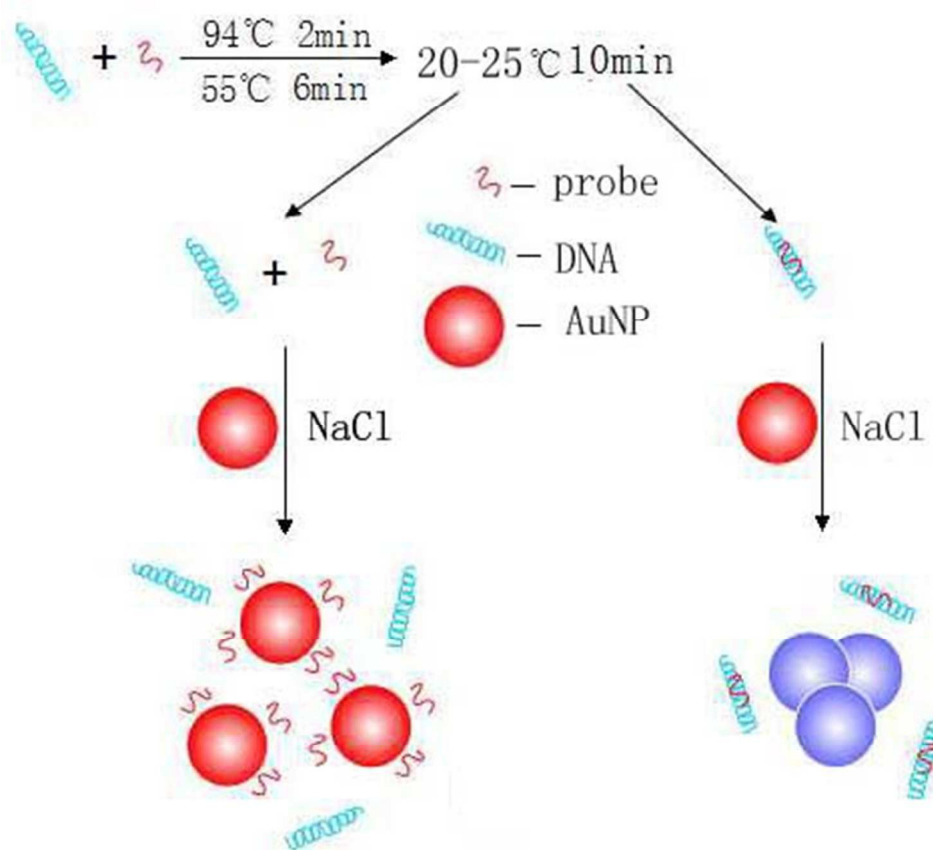
Scheme 1. Schematic illustration for visual detection of MCMV based on unmodified AuNPs

Fig.1 Verification experiment for visual detection strategy of MCMV. (A) Visual color changes of AuNPs upon the addition of various genomic sequences; (B) UV-vis absorption spectra of different state of AuNPs; (C) Transmission electron microscopy of different state of AuNPs. (a) 13 nm AuNPs; (b) 13 nm AuNPs, target (RT-PCR product from MCMV) and probes after saline induction; (c) 13 nm AuNPs, the 289-bp fragments from *Staphylococcus aureus* and probes after saline induction.

Fig. 2 Critical NaCl concentration for the color change of existing status of AuNPs collides. 35 μ L of mixtures (containing 0.1 μ L DNA or distilled water, 1 μ L of 10 μ M probes, 30 μ L of AuNPs, and some distilled water) was subjected to denaturation at 95 $^{\circ}$ C for 2 min, annealing at 55 $^{\circ}$ C for 6min, and then cooling to room temperature for 10 min before adding different concentration of NaCl induction for 90 min. No.1 was distilled water as control; No.2 was 476-bp RT-PCR of MCMV RNA; No.3 was the 289-bp PCR of *Staphylococcus aureus*; No.4 was 226-bp PCR of *Listeria monocytogenes*; (A) 40 mM NaCl; (B) 50 mM NaCl; (C) 60 mM NaCl; (D) 65 mM NaCl.

Fig. 3 Specificity of visual detection of MCMV. (A) Electrophoresis of RT-PCR products from different virus and control. M was the DNA ladder; Lane 1-8 represented MCMV-1087, MCMV-C2094, MCMV-C1907, MCMV-C2219, MCMV-V219-P1, MCMV-ZJ, MCMV-BJ and MCMV, respectively; lane 9 was distilled water; Lane 10-16 represented CRSV, ORSV, CGMMV, LSV, CymMV, SBMV and BPMV, respectively; (B) Different results of RT-PCR combination with a species-specific probe after salt induction. Lane 0 was distilled water and used as control, others are the same as to Fig.3A.

Fig.4 Sensitivity of visual detection of RNA of MCMV. (A) M: 2000 bp DNA ladder; lane 1: 2.4 ng/ μ L; lane 2 : 0.24 ng/ μ L; lane 3: 0.12 ng/ μ L; lane 4: 60 pg/ μ L; lane 5: 30 pg/ μ L; lane 6: 15 pg/ μ L; lane 7: 7.5 pg/ μ L; lane 8: 3.75 pg/ μ L; lane 9:1.875 pg/ μ L; Lane 10: distilled water.



Scheme 1. Schematic illustration for visual detection of MCMV based on unmodified AuNPs
125x112mm (96 x 96 DPI)

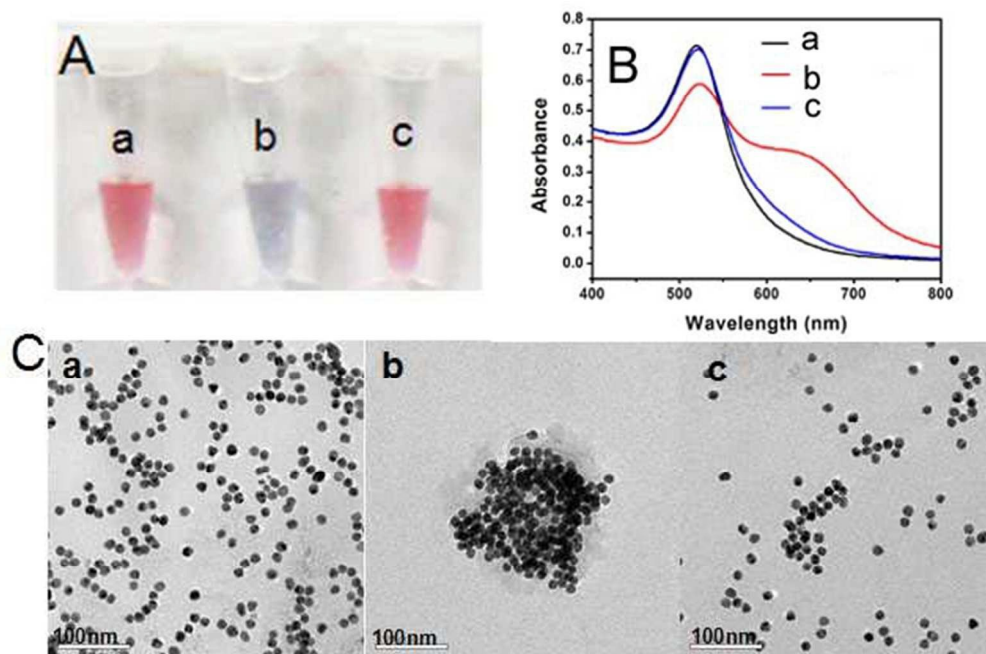


Fig.1 Verification experiment for visual detection strategy of MCMV. (A) Visual color changes of AuNPs upon the addition of various genomic sequences; (B) UV-vis absorption spectra of different state of AuNPs; (C) Transmission electron microscopy of different state of AuNPs. (a) 13 nm AuNPs; (b) 13 nm AuNPs, target (RT-PCR product from MCMV) and probes after saline induction; (c) 13 nm AuNPs, the 289-bp fragments from *Staphylococcus aureus* and probes after saline induction.
168x110mm (96 x 96 DPI)

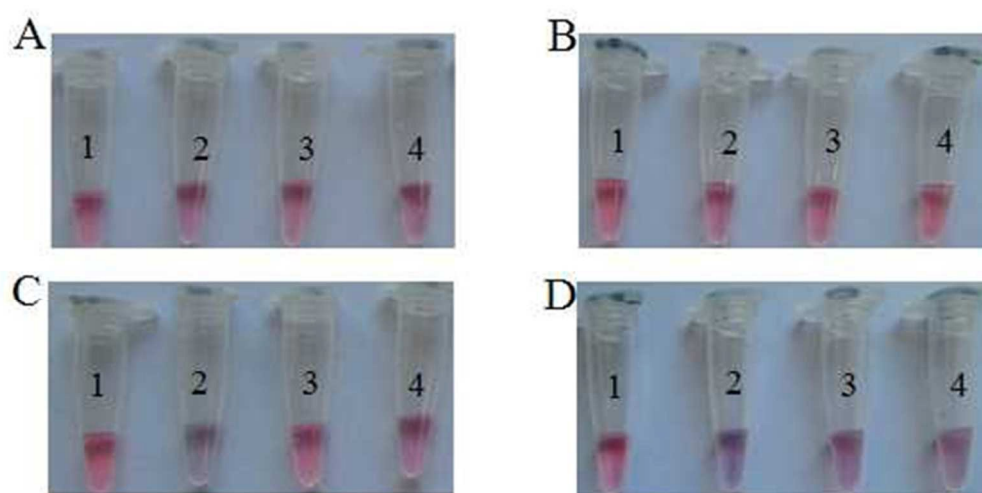


Fig. 2 Critical NaCl concentration for the color change of existing status of AuNPs collides. 35 μ L of mixtures (containing 0.1 μ L DNA or distilled water, 1 μ L of 10 μ M probes, 30 μ L of AuNPs, and some distilled water) was subjected to denaturation at 95 $^{\circ}$ C for 2 min, annealing at 55 $^{\circ}$ C for 6min, and then cooling to room temperature for 10 min before adding different concentration of NaCl induction for 90 min. No.1 was distilled water as control; No.2 was 476-bp RT-PCR of MCMV RNA; No.3 was the 289-bp PCR of *Staphylococcus aureus*; No.4 was 226-bp PCR of *Listeria monocytogenes*; (A) 40 mM NaCl; (B) 50 mM NaCl; (C) 60 mM NaCl; (D) 65 mM NaCl.
137x69mm (96 x 96 DPI)

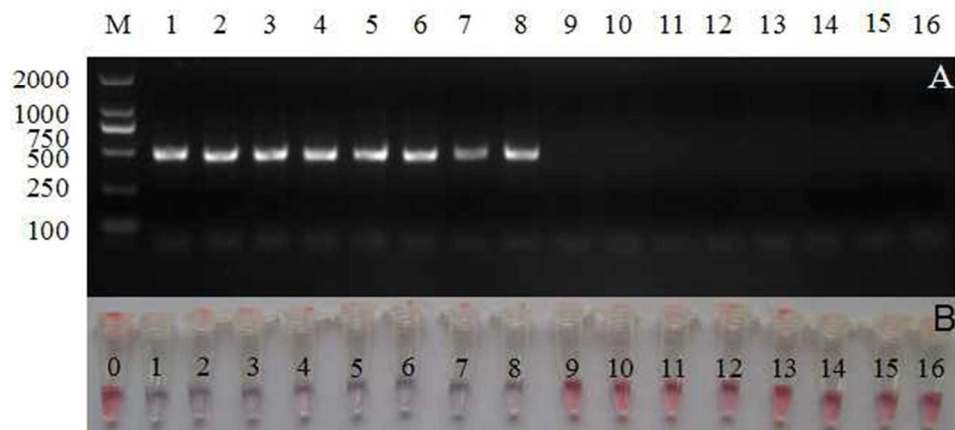


Fig. 3 Specificity of visual detection of MCMV. (A) Electrophoresis of RT-PCR products from different virus and control. M was the DNA ladder; Lane 1-8 represented MCMV-1087, MCMV-C2094, MCMV-C1907, MCMV-C2219, MCMV-V219-P1, MCMV-ZJ, MCMV-BJ and MCMV, respectively; lane 9 was distilled water ; Lane 10-16 represented CRSV, ORSV, CGMMV, LSV, CymMV, SBMV and BPMV, respectively; (B) Different results of RT-PCR combination with a species-specific probe after salt induction. Lane 0 was distilled water and used as control, others are the same as to Fig.3A.

174x76mm (96 x 96 DPI)

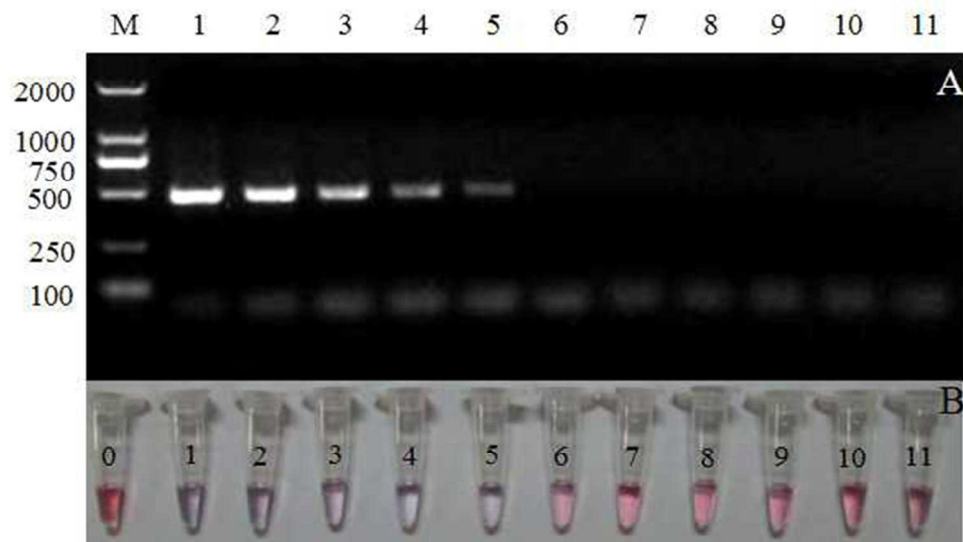


Fig.4 Sensitivity of visual detection of RNA of MCMV. (A) M: 2000 bp DNA ladder; lane 1: 2.4 ng/ μ L; lane 2 : 0.24 ng/ μ L; lane 3: 0.12 ng/ μ L; lane 4: 60 pg/ μ L; lane 5: 30 pg/ μ L; lane 6: 15 pg/ μ L; lane 7: 7.5 pg/ μ L; lane 8: 3.75 pg/ μ L; lane 9:1.875 pg/ μ L; Lane 10: distilled water.
161x88mm (96 x 96 DPI)